Direct Observation of Desorption Kinetics with Perylene at Ultrafine Aerosol Particle Surfaces

Ch. Hueglin, J. Paul, L. Scherrer, and K. Siegmann*

Laboratory for Solid State Physics, ETH Zurich, 8093 Zurich, Switzerland

Received: June 30, 1997; In Final Form: September 9, 1997[⊗]

A new method for the investigation of the desorption dynamics from ultrafine particle surfaces is presented. It uses photoelectric charging of the substrate particles by a pulsed light source. The yield of such charging near photoelectric threshold depends on the state of the surface with submonolayer sensitivity. If the substrate particles are suspended in a gas at ambient conditions, a time resolution of a few milliseconds is achieved. As an example, we measured the thermal desorption of perylene ($C_{20}H_{12}$) from sodium chloride (NaCl) and carbon particles. The first-order rate constant of perylene desorption from NaCl particles was determined for temperatures between 66.3 and 86.0 °C. The time required for the reduction of the perylene concentration to 1/e of the initial value was found to be $t_d = 396$ ms for $T = 66.3$ °C and $t_d = 36$ ms for $T = 86.0$ °C. The desorption activation energy was determined to $E_d = 122.9(3.0)$ kJ/mol. This value is in excellent agreement with the result obtained by an equilibrium method and taken from the literature.[1] Thermal desorption of perylene from the surface of carbon particles was studied for temperatures between 67.5 and 104.5 °C. The obtained time constants are larger than for NaCl particles. (At $T = 83.0$ °C the time constant is $t_d = 94$ ms compared to $t_d = 54$ ms for perylene desorption from NaCl particles.) Thermal desorption from carbon particles cannot be explained in terms of a single desorption activation energy. The experimental data are interpreted as desorption from a distribution of adsorption sites with different desorption activation energies.

1. Introduction

The investigation of desorption processes is a wide and important field in surface sciences. The dynamics of desorption depends on the mechanism of the energy transfer to the desorbing species. The energy necessary for desorption can be provided from the substrate or from external sources such as photons or electron and ion beams. If the substrate acts as a heat reservoir from which the energy is taken, the process is called thermal desorption. The experimental techniques for the investigation of adsorbate/surface interactions usually rely on a high-vacuum environment. In this work, we report on a measuring principle that is based on aerosol techniques and that is applied to ultrafine particles suspended in a gas at room temperature and atmospheric pressure. Measuring techniques that allow to study adsorbate/surface interactions or more general heterogeneous and multiphase reactions under ambient conditions are highly desired because those processes play a major role in the chemistry of the atmosphere.[2]

The apparatus built for the time-resolved investigation of adsorption and desorption processes and of chemical reactions on aerosol particle surfaces is described. The underlying idea is to transfer the aerosol under investigation rapidly into a new environment where the reaction is initiated at a well-defined moment. This new environment may contain reactive or adsorbing compounds or may simply be of elevated temperature as in the experiments presented here. The first-order kinetics of thermal desorption of perylene ($C_{20}H_{12}$) from the surface of different substrate particles was investigated, and the desorption activation energies were determined. Perylene was used as the adsorbate because of the following reasons: It is a nontoxic representative of the class of polycyclic aromatic hydrocarbons (PAHs), which are byproducts of incomplete combustion processes and considered as hazardous ambient trace substances[3] which are present as volatile, semivolatile, and particulate pollutants.[4,5] Perylene is an isomer of the well-known carcinogen benzo[*a*]pyrene which was recently linked to the development of lung cancer on a molecular basis.[6] Moreover, perylene is entirely particle bound at ambient temperature and causes a large increase of the photoelectric yield of the particles upon adsorption. This photoelectric yield enhancement is well-known for surfaces that are covered at levels at or below a monolayer of PAHs and is used in photoelectric aerosol sensors for the continuous detection of particle bound PAHs.[7] Different physical mechanisms that can explain this unusual yield enhancement are discussed by Greber et al.[8]

Sodium chloride (NaCl) particles as well as carbon particles were used as substrates. These particles have been chosen because of their different geometrical shape and their relevance for the atmospheric aerosol. Sodium chloride particles are mainly formed by sea spray; carbon particles resemble the soot particles produced in the combustion of organic fuels.

2. Theory

The simplest description of desorption is given by an Arrhenius type reaction law. The rate of desorption of a molecule A is written as

$$r_d = -\mathrm{d[A]}/\mathrm{d}t = \nu[\mathrm{A}]^x \exp(-E_d/RT) \qquad (1)$$

where [A] is the concentration of molecules in the adsorbed state, ν is the preexponential factor, x is the reaction order, R is the gas constant, and E_d is the desorption activation energy (which is equal to the binding energy for a nonactivated desorption process). Equation 1 is called Frenkel−Arrhenius or Polanyi−Wigner Equation.[9,10] The preexponential factor contains dynamical information about the desorption process. It is often interpreted as the attempt frequency with which an adsorbed molecule tries to escape from the surface and therefore

* Corresponding author. email: k.siegmann@solid.phys.ethz.ch. Tel. (+41) 1 633 6832, FAX (+41) 1 633 1080.

[⊗] Abstract published in *Advance ACS Abstracts,* October 15, 1997.

S1089-5647(97)02104-4 CCC: $14.00

estimated to be of the order of 10^{12} s^{-1}. The desorption activation energy and the preexponential factor are assumed to be independent of temperature and surface coverage. The reaction order x is one for desorption of intact molecules. (Desorption with $x = 0$ might be observed at multilayer coverages, when the number of desorbing molecules is small compared to the total number of molecules in the adsorbed state.) For a first-order reaction ($x = 1$), the solution of eq 1 is

$$[\mathrm{A}](t) = [\mathrm{A}]_0 \exp(-k_\mathrm{d} t) \tag{2}$$

with

$$k_\mathrm{d} = \nu \exp(-E_\mathrm{d}/RT) \tag{3}$$

k_d is the rate constant of the reaction.

For desorption from aerosol particles, readsorption of the desorbing molecules by diffusion must be taken into account. Therefore, a probability factor p is multiplied to the right (hand) side of eq 1. This factor stands for the desorption probability; it is $p = 1$ if no reabsorption occurs and $p = 0$ when every desorbing molecule is recaptured ($0 \leq p \leq 1$).

An expression for the probability factor has been derived. We consider a spherical particle with radius r_p as the source of desorbing molecules. In a distance r from the particle origin the molecular flux through a unit surface can be written as the current density $j(r)$. It is assumed that the molecules thermalize in a distant δ from the particle surface. The magnitude of δ is given by $\delta = R - r_\mathrm{p}$, where R is the radius of the so-called limiting sphere. The concept of the limiting sphere is due to Fuchs[11] and Wright.[12] It serves as the boundary between the continuum regime and the molecular regime. Outside the limiting sphere, the motion of gas molecules is considered as diffusive (continuum regime); inside the sphere the gas molecules follow trajectories that are described by kinetic theory (molecular regime). From the surface of the limiting sphere the thermalized molecules are assumed to move randomly in either direction. Therefore, the total molecular flux at the surface of the limiting sphere will be given by the sum of an outward ($j_\mathrm{out}(R)$) and an inward flux ($j_\mathrm{in}(R)$). The desorption probability p is defined as

$$p = \frac{j_\mathrm{out}(R) + j_\mathrm{in}(R)}{j_\mathrm{out}(R)} \tag{4}$$

Starting from Fick's first law of diffusion the calculation of p is straightforward and yields

$$p = \left(1 + \frac{r_\mathrm{p}}{R}\,\eta\,\frac{1}{\pi^{1/2} K_n}\right)^{-1} \tag{5}$$

where η is the sticking probability defined as the ratio of the number of surface collisions resulting in an adsorbed state and the number of molecules that impinge on the surface. Furthermore, K_n is the Knudsen number ($K_n = \lambda/r_\mathrm{p}$, λ is the mean free path). If the particle size is known, the radius of the limiting sphere is determined according to Wright,[12] and the Knudsen number can be calculated. However, sticking probabilities are generally unknown. There are only few experimental data on sticking probabilities of interactions between molecules and aerosol particles available from the literature. For example, Fendel et al.[13] determined the sticking probability for ozone on ultrafine carbon and iron aerosol particles; Kalberer et al.[14] measured the sticking probability for the adsorption of $^{13}NO_2$ onto ultrafine carbon particles. In both measurements, sticking probabilities of the order of 10^{-4} were obtained. In Table 1 desorption probability factors for a selection of different Knudsen numbers and sticking probabilities are shown. The experiments presented in this work were carried out under conditions with Knudsen numbers larger than one and approximately equal to one. It is expected that the sticking probabilities are much smaller than one, and the desorption probabilities are therefore very close to unity.

TABLE 1: Desorption Probability Factors for Different Particle Sizes and Sticking Probabilities as Obtained from Eq 6[a]

d_p (nm)	K_n	$p(\eta=1)$	$p(\eta=0.1)$	$p(\eta=0.01)$
5	13	0.997	1.000	1.000
65	1	0.764	0.970	0.997
500	0.13	0.201	0.715	0.962
5000	0.013	0.023	0.189	0.699

[a] The mean free path was assumed to be $\lambda = 65$ nm, corresponding to the mean free path in air at normal atmospheric conditions.[15] The desorption probability factor is $p = 1$ if no readsorption occurs and $p = 0$, when every desorbed molecule is recaptured.

3. Experimental Section

The experimental setup consists of a particle generation section, a particle coating section, and the desorption unit. As substrate particles, ultrafine sodium chloride and carbon particles were used. The NaCl particles were generated by atomization of a 2% aqueous solution followed by a diffusion drier whereas the carbon particles were produced by a spark discharge aerosol generator[16] operated with nitrogen as carrier gas (99.999% purity). The mean particle mobility diameter was about 25 nm (carbon particles) and about 90 nm (NaCl particles), respectively. Both particle types are of different geometry as revealed by scanning electron microscopy (Figure 1). NaCl particles are crystalline cubes with smooth surfaces, whereas carbon particles are formed by aggregation of primary particles and of irregular structure. The fractal-like dimension of carbon particles from a spark discharge generator was found to be between 2.05 and 2.35.[18]

In a following coating section, the substrate particles were coated with a thin layer of perylene. Subsequently, the particles entered the desorption unit which is based on an aerosol diluter described by Hueglin et al.[19] connected to a photoemission tube (Figure 2). In the desorption unit a small portion of the coated particles was rapidly transferred from ambient temperature (T_0) into a particle-free gas stream in a heatable tube at a temperature of T_1. The particle transfer is carried out by a rotating disk which contains a single cavity with a volume of about 40 mm^3. The cavity is positioned over the aerosol channel and therefore filled with a small portion of coated particles. Driven by a step motor, the disk can be triggered for one full turn. At a rotation angle of 180° the cavity passes over a second channel, where particle free air at temperature T_1 flows. In this position, the cavity is exposed to the gas stream for about 5 ms. Consequently, the particle portion is flushed out of the cavity and injected into the photoemission tube. Because of their low heat capacity the particles attain very rapidly the temperature of the carrier gas (T_1). The time of particle injection therefore set the well-defined starting point for the desorption process ($t = 0$). Readsorption is quenched, because the injection leads to a high dilution of the aerosol portion. Consequently, the partial pressure of the gaseous perylene in the photoemission tube is very small, which creates a nonequilibrium situation. Inside the photoemission tube, the particles are irradiated with a single excimer-laser pulse (wavelength $\lambda = 193$ nm) of 20 ns duration, charging the particles photoelectrically. Because of their high electrical mobility, the electrons and negatively charged ions

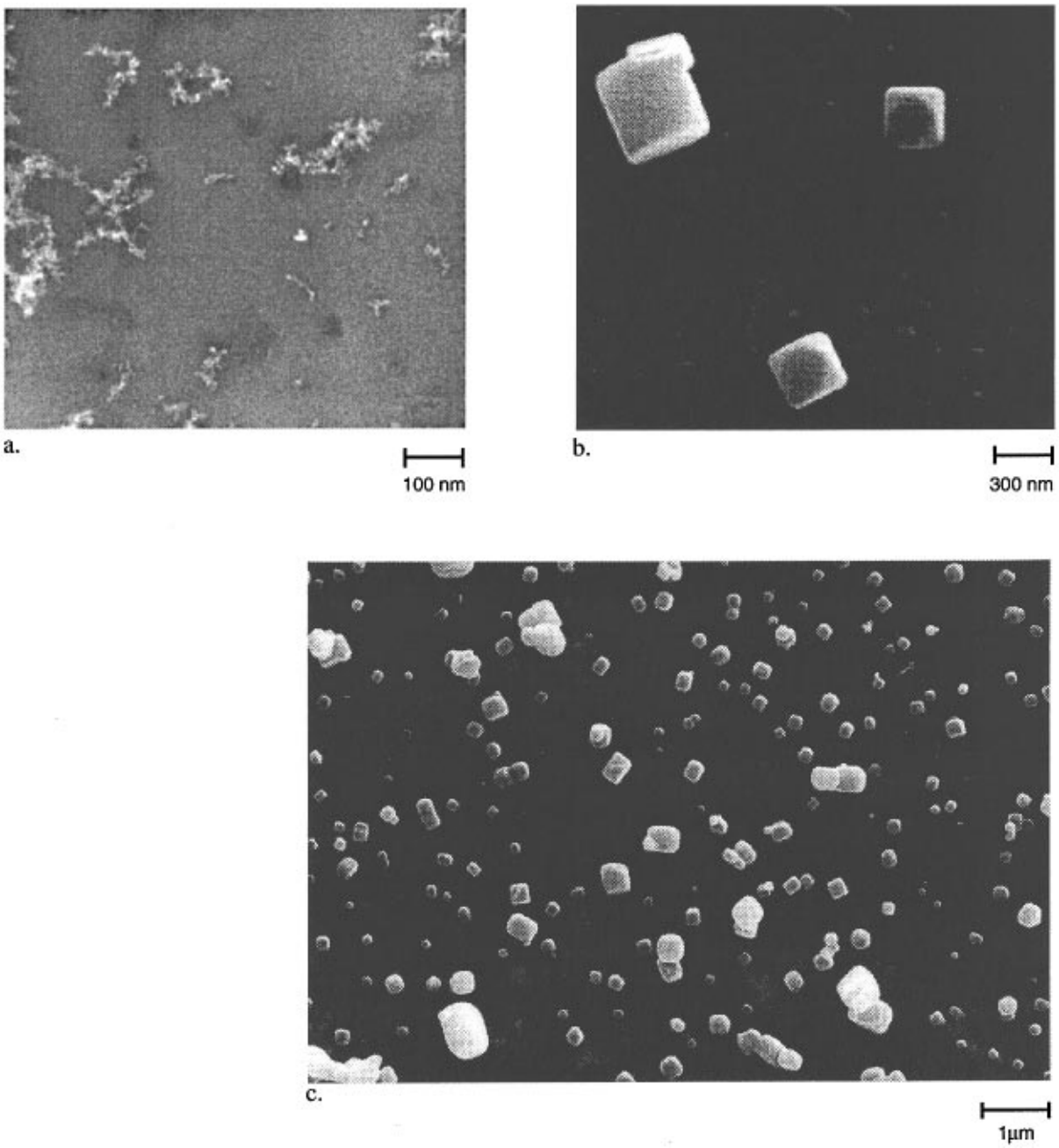

Figure 1. Scanning electron micrographs of polydisperse carbon particles produced by a spark discharge generator (a) (taken from ref 17) and polydisperse sodium chloride particles generated by atomization of a 2% aqueous solution (b and c). The sodium chloride particles are covered with a thin layer of perylene.

(generated due to capture of the electrons by air molecules) can be selectively precipitated in a small alternating electric field. The time-averaged motion of the positive charged particles remains unaffected by the small field. At the outlet of the photoemission tube, the total particle charge is measured by integrating the output of a current amplifier. For a thin coating of the particle surface, the measured total photoelectric charge is proportional to the number of perylene molecules in the adsorbed state.[20]

The particle portions are illuminated by single UV-laser pulses at different times with respect to the particle injection ($t = 0$ at the injection). The recorded total particle charge corresponds to the number concentration of adsorbed perylene molecules at the time of particle illumination. By evaluation of the number concentration of adsorbed perylene molecules as a function of time, the kinetics of the desorption process can be followed. In the presented experiments, eight measurements for every selected delay time have been carried out, and the arithmetic mean was determined. The accessible time ranges from 0 to 1200 ms. However, the data points with delay times shorter than 50 ms shows a large standard deviation due to the mixing process of particles and dilution gas.

The linear relationship between photoemission signal and number of adsorbed perylene molecules is only valid for low laser intensities. In a separate experiment, the total photoelectric charge (denoted as photoemission signal (PE)) was measured as a function of the light intensity. The observed functional dependence was used to correct the photoemission signal for the shot-to-shot instability and long-term drifts of the laser intensity (LI). The laser intensity was adjusted so that the average particle charge was approximately unity for particles with the initial perylene coating. A fraction of the flow of coated particles was directed to a photoelectric aerosol sensor (PAS)[7] in order to record instabilities of the particle generation

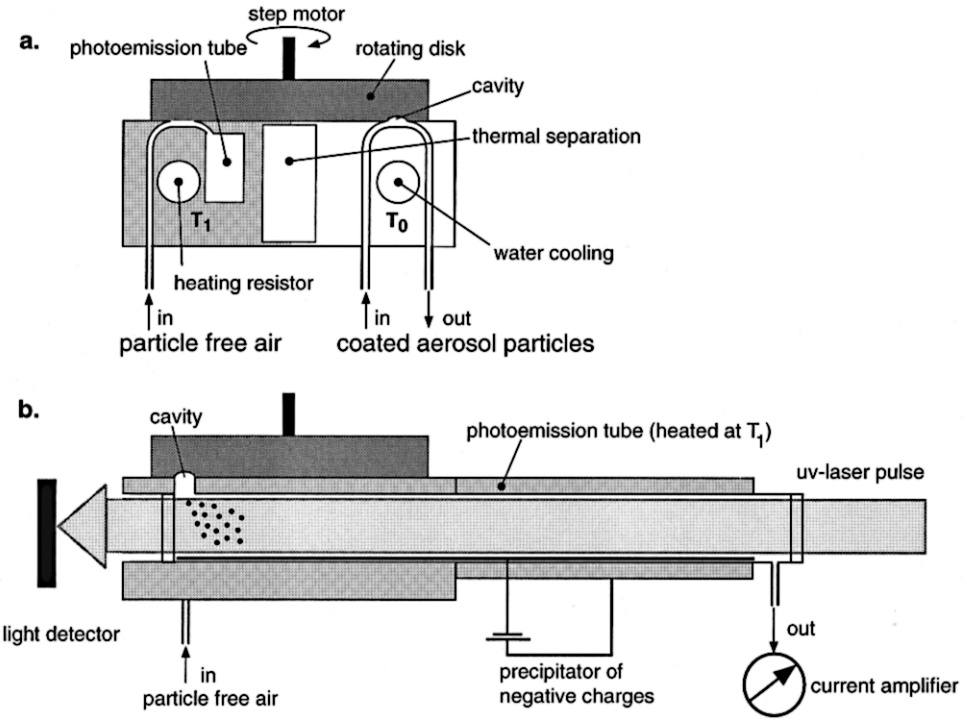

Figure 2. Schematic of the experimental setup: (a) front view and (b) side view. The region near the coated particle flow can be cooled (25 °C $\leqslant T_0 \leqslant$ 35 °C), whereas the region near the dilution gas flow can be heated (25 °C $\leqslant T_1 \leqslant$ 120 °C). Both regions are thermally isolated. As illustrated in (b), the photoemission tube is kept at temperature T_1 by an electronically controlled heating.

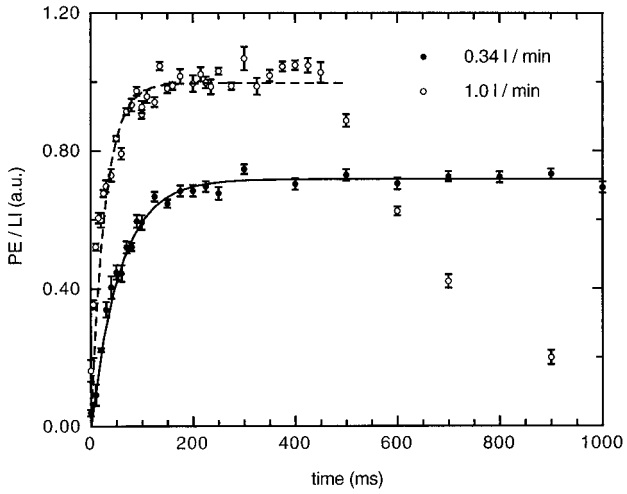

Figure 3. Photoemission signal (PE) of carbon particles coated with perylene as a function of delay time. PE was normalized to the laser intensity (LI). Data for two different flow rates at $T_0 = T_1 = 25$ °C are shown. At this temperature, the desorption rate of perylene is very low. Therefore, the propagation of the particles through the photoemission tube is shown.

and coating section. The photoemission signal was divided by the PAS signal to compensate for those instabilities. In the measurements, the time between particle injection and the end of the data acquisition was typically 8 s. This time consumption for one cycle is mainly due to the low flow rate in the photoemission tube and the time constant of the current amplifier.

Figure 3 shows the photoemission signal of carbon particles coated with perylene as a function of delay time. The photoemission signal was normalized to the laser intensity. Curves for two different flow rates (0.34 and 1.0 L/min) in the photoemission tube kept at ambient temperature ($T_1 = T_0 = 25$ °C) are shown. At this conditions, the desorption rate of perylene is very small; the graph therefore shows the propagation of the particle portion along the photoemission tube. At $t = 0$ ms, the particles are injected into the tube; the signal increases steeply and reaches constant values at about 100 and 200 ms, respectively. For a flow rate of 1.0 L/min the photoemission signal starts to decrease at 500 ms because the first particles of the diffusively broadened particle pulse are leaving the tube. The curves are reproducible within an accuracy of about 10% in the increasing region and better than 5% in the constant region. These data serve for normalization of the desorption data. A time resolution of a few milliseconds is achieved with this setup. The photoemission signal is larger for a flow rate of 1.0 L/min than for 0.34 L/min. It is assumed that the aerosol portion was not completely flushed into the dilution gas at the lower flow rate. Measurements with flow rates higher than 1.0 L/min did not show a further increase of the signal. This situation has only the consequence of a lower signal-to-noise ratio. The results presented in the following were obtained with a flow rate of 0.34 L/min.

4. Results

Thermal desorption of perylene from NaCl particles was measured for different temperatures T_1 in the range between 66.3 and 86.0 °C (Figure 4). The measured desorption data were corrected by the particle propagation curve from Figure 3. Exponential curves with three parameters were fitted to the data. The interception with the y axis (PE/LI ($t = 0$)), the exponential factor, and a constant offset were floating fit parameters. The offset results from a small photoelectric activity of the uncoated particles. Only the data points with delay times equal or larger than 50 ms have been used for evaluation of the data, because the measurements with shorter delay times showed a high variation of the signal due to the particle injection process.

From the exponential factors the temperature-dependent rate constants k_d were determined (eq 3). The kinetics of perylene desorption from NaCl particles is well-described by eq 3, it is therefore considered a first-order process. The time constants of the desorption process are given by k_d^{-1} and were found to

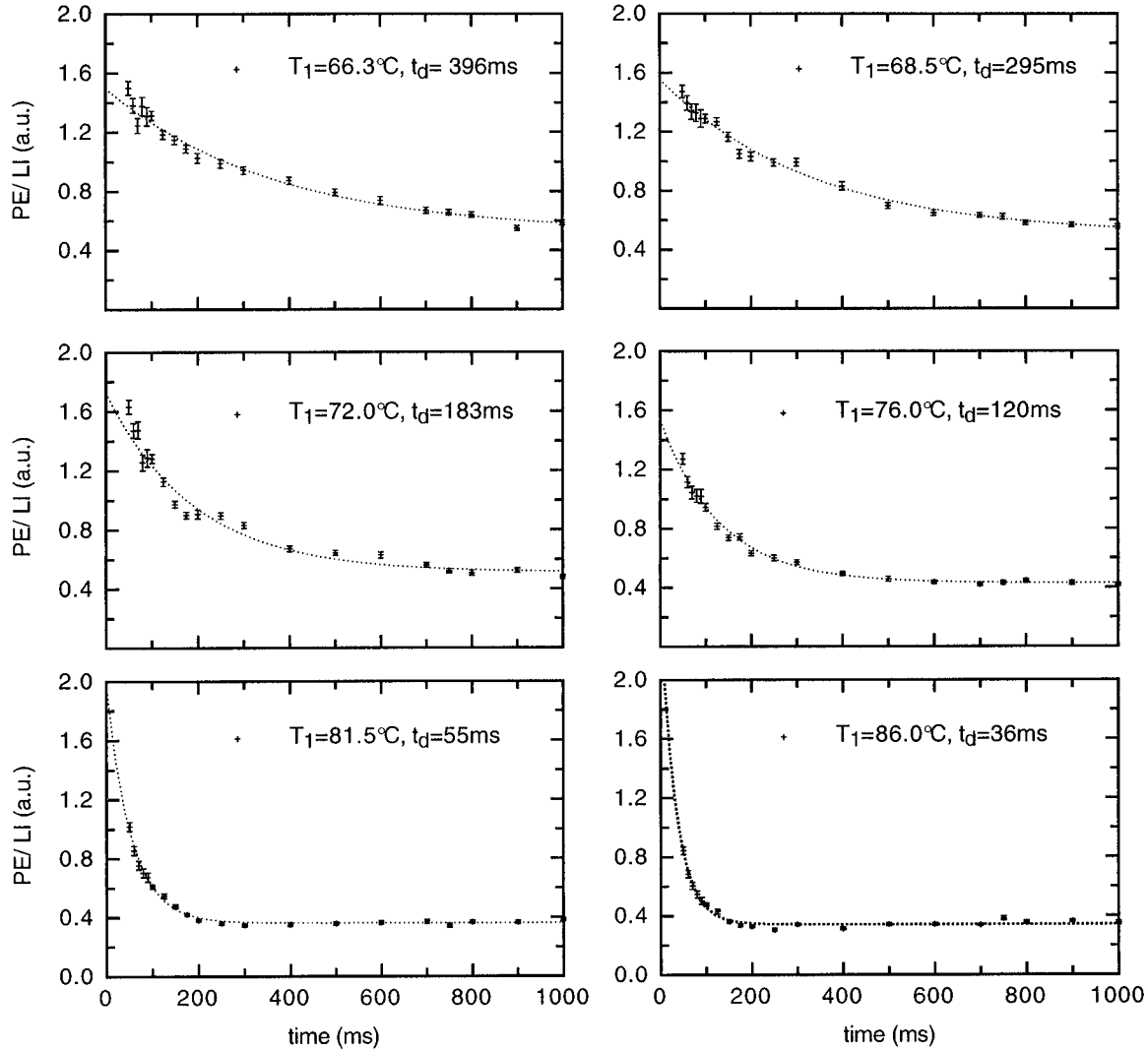

Figure 4. Desorption of perylene from polydisperse NaCl particles (mean particle diameter of 90 nm) at various temperatures. Exponential curves were fitted to the data (dotted lines).

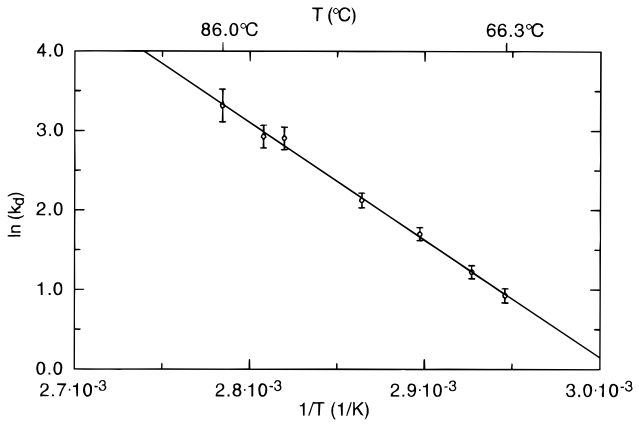

Figure 5. Temperature dependence of the rate constant in Arrhenius representation. From the slope of the regression line the desorption activation energy was evaluated to $E_d = 122.9(3.0)$ kJ/mol. The intersection with the *y* axis gives the logarithm of the preexponential factor. The preexponential factor was determined to $\nu = 2.1 \times 10^{19}$ (1.1×10^{18}) s^{-1}.

be $t_d = 396$ ms for $T_1 = 66.3$ °C and $t_d = 36$ ms for $T_1 = 86.0$ °C. Figure 5 illustrates the temperature dependence of the rate constant in Arrhenius representation. From the slope of the linear regression, the desorption activation energy was determined to $E_d = 122.9(3.0)$ kJ/mol. This desorption activation energy is in excellent agreement with the value obtained by Steiner and Burtscher[1] (123 kJ/mol). In these measurements an equilibrium method was used to study perylene desorption from monodisperse NaCl particles with diameters of 60 nm. The preexponential factor can be determined from the intersection with the *y* axis. A value of $\nu = 2.1 \times 10^{19}$ (1.1×10^{18}) s^{-1} was obtained. Such high preexponential factors are in contradiction to the interpretation as vibrational attempt frequencies but have been observed in various unimolecular desorption processes.[21] However, there are still open questions how preexponential factors of such magnitudes might be explained.

Desorption of perylene from irregularly shaped carbon particles was studied for temperatures between 67.5 and 104.5 °C. Figure 6 shows the desorption curves for various measurements. They look similar to the data presented for desorption from NaCl particles. Again, exponential curves were fitted to the desorption data, and the first-order rate constants were determined. For a given temperature, the rate constants are smaller than in the NaCl measurements. At $T_1 = 83.0$ °C, the time constant was $t_d = 94$ ms compared to $t_d = 54$ ms for desorption from NaCl particles. Figure 7 shows the obtained rate constants in the Arrhenius representation. Determination of the slope of the linear regression gives a desorption activation energy of $E_d = 67.7(6.8)$ kJ/mol. This value is much lower than the literature value of 133 kJ/mol.[1] We conclude that the simple Arrhenius law is not applicable to describe the desorption from the surface of carbon particles. If perylene desorption from

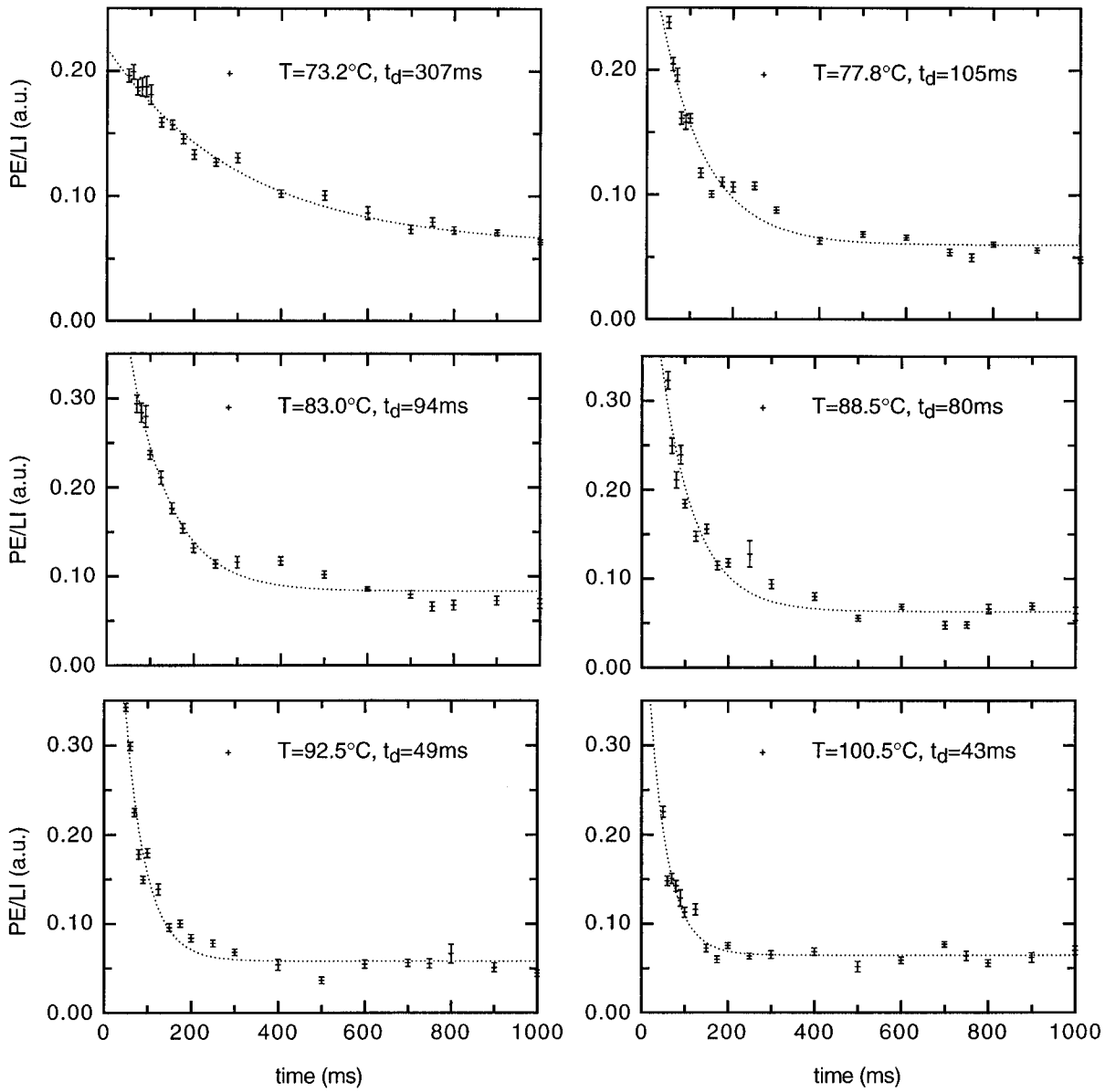

Figure 6. Desorption of perylene from polydisperse carbon particles (mean diameter of 25 nm) at various temperatures. Exponential curves were fitted to the data (dotted lines).

carbon particles is considered to be a first-order process, it cannot be explained in terms of a single desorption activation energy. This result is regarded as a consequence of the irregular particle structure.

However, the experimental data can qualitatively be described by a simple model, where two adsorption sites with slightly different desorption activation energies are assumed. We consider adsorption sites with a desorption activation energy E_d as obtained from the NaCl measurement (denoted as $E_{d(NaCl)}$) and adsorption sites that are stronger bound by 4% ($E_d = 1.04E_{d(NaCl)}$). It is further assumed that both sites are equally populated and that the preexponential factors are similar for both sites and equal to the value found for perylene desorption from NaCl particles. The expected desorption curves for this situation were calculated and evaluated by means of a single-exponential function. This results in a temperature dependence of the rate constant as included in Figure 7 (curve denoted as "model"). The misfit of the Arrhenius law is consequently the result of the approximation of a sum of two exponential functions by a single-exponential function.

Consider the rate constant for desorption from the sites with lower activation energy to be k_{d1} and the rate constant for desorption from the sites with higher activation energy to be k_{d2}. At low temperatures, the rate constant is dominated by desorption from the sites with the lower activation energy. If the desorption data are then described by means of a single-exponential function, a value close to k_{d1} is obtained. At a higher temperature, the loosely bound sites will be completely depopulated, and desorption occurs only from the more strongly bound sites. The observed desorption will therefore be dominated by the slower process. Then, the rate constant observed by our method is equal to k_{d2}. In the temperature region between these extremes a rate constant that is smaller than k_{d1} but larger than k_{d2} is obtained when a single-exponential function is fitted to the data. As mentioned before, this model is a simplification because it only considers two types of adsorption sites. The desorption activation energies considered in this model have been chosen somewhat arbitrarily in order to describe the desorption process as observed in the experiment. However, it leads us to the assumption that a variety of adsorption sites with specific desorption activation energies are available on the surface of carbon particles.

The existence of a distribution of different adsorption sites on the surface of carbonaceous particles was also suggested in

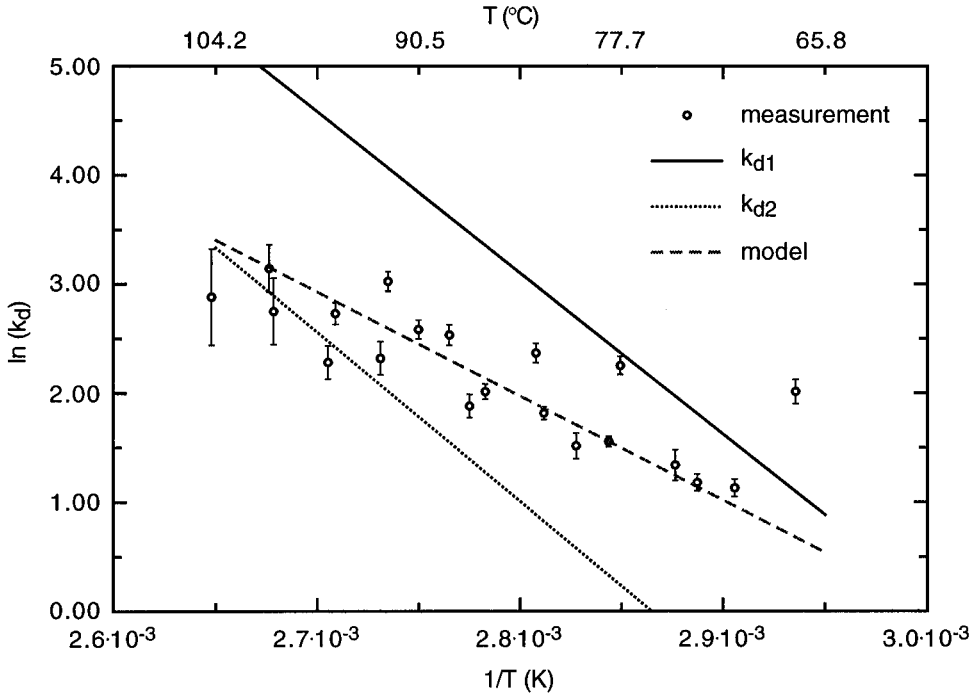

Figure 7. Temperature dependence of the measured rate constant of perylene desorption from carbon particles (open circles). The experimental data can qualitatively be described by assumption of two types of equally populated adsorption sites with different desorption activation energies. Adsorption sites with an E_d as observed from the NaCl measurement, denoted as k_{d1} (solid line), and adsorption sites which are stronger bound by 4%, denoted as k_{d2} (dotted line), were assumed. The preexponential factors for both types of sites were assumed to be equal and also taken from the NaCl measurement. The result expected for this situation is shown by the broken line (see text for discussion).

earlier nonkinetic studies. Steiner and Burtscher[1] stated that this assumption is more adequate for the interpretation of perylene desorption from carbon and diesel soot particles than the consideration of a sharp desorption activation energy. In addition, a different desorption behavior of radiochemically labeled ^{136}I, ^{86}Br, and ^{13}NO from carbon particles compared to desorption from silver particles was observed.[22] There, it was assumed that either a strong entropy contribution to the desorption reaction or a broad distribution of chemically different adsorption sites on the particle surface is responsible for the differences.

5. Conclusions

A new method for the direct observation of the desorption from ultrafine particle surfaces at room temperature and atmospheric pressure is presented. The kinetics of thermal perylene desorption from NaCl and carbon particles was measured with a time resolution of a few milliseconds. It is shown that the desorption process from NaCl particles follows a first-order rate law. The Arrhenius model is suited to describe this desorption. Desorption of perylene from carbon particles cannot be explained by desorption from a single type of adsorption site. It is suggested that a distribution of adsorption sites with different desorption activation energies is present on the surface of irregularly shaped carbon particles. A variety of open questions concerning gas/particle interactions might be addressed with the experimental method introduced here. As an example, the work of Weingartner et al.[17,23] on the hygroscopic behavior of combustion aerosol particles could be extended in terms of the kinetics of the water uptake.

Acknowledgment. We thank H. C. Siegmann for inspiring discussions, A. V. Filippov for his suggestions regarding the desorption probability factor, and P. Wägli for carrying out the electron microscopic analysis.

References and Notes

(1) Steiner, D.; Burtscher, H. *Environ. Sci. Technol.* **1994**, *28*, 1254.
(2) Ravishankara, A. R. *Science* **1997**, *276*, 1058 and references therein.
(3) Grimmer, G., Ed. *Environmental Carcinogens: Polycyclic Aromatic Hydrocarbons: Chemistry, Occurrence, Biochemistry, Carcinogenicity*; CRC Press: Boca Raton, FL, 1983.
(4) Yamasaki, H.; Kuwata, K.; Miyamoto, H. *Environ. Sci. Technol.* **1982**, *16*, 189.
(5) Allen, J. O.; Dookeran, N. M.; Smith, K. A.; Sarofim, A. F.; Taghizadeh, K.; Lafleur, A. L. *Environ. Sci. Technol.* **1996**, *30*, 1023.
(6) Denissenko, M. F.; Pao, A.; Tang, M.; Pfeifer, G. P. *Science* **1996**, *274*, 430.
(7) Burtscher, H. *J. Aerosol Sci.* **1992**, *23*, 549.
(8) Greber, T.; Giessel, T.; Pettenkofer, C.; Siegmann, H. C.; Ertl, G. *Surf. Sci.* **1995**, *343*, L1187.
(9) Frenkel, J. *Z. Phys.* **1924**, *26*, 117.
(10) Ehrlich, G. *J. Appl. Phys.* **1961**, *32*, 4.
(11) Fuchs, N. A. *The Mechanics of Aerosols*; Pergamon Press: Oxford, 1964.
(12) Wright, P. G. *Faraday Discuss.* **1960**, *30*, 100.
(13) Fendel, W.; Matter, D.; Burtscher, H.; Schmidt-Ott, A. *Atmos. Environ.* **1995**, *29*, 967.
(14) Kalberer, M.; Ammann, M.; Tabor, K.; Parrat, Y.; Weingartner, E.; Piguet, D.; Rössler, E.; Jost, D. T.; Türler, A.; Gäggeler, H. W.; Baltensperger, U. *J. Phys. Chem.* **1996**, *100*, 15487.
(15) Hinds, W. C. *Aerosol Technology;* John Wiley & Sons: New York, 1982.
(16) Schwyn, S.; Garwin, E.; Schmidt-Ott, A. *J. Aerosol Sci.* **1988**, *19*, 639.
(17) Weingartner, E.; Burtscher, H.; Baltensperger, U. *Atmos. Environ.* **1997**, *31*, 2311.
(18) Schleicher, B.; Künzel, S.; Burtscher, H. *J. Appl. Phys.* **1995**, *78*, 4416.
(19) Hueglin, Ch.; Scherrer, L.; Burtscher, H. *J. Aerosol Sci.* **1997**, *28*, 1049.
(20) Niessner, R.; Wilbring, P. *Anal. Chem.* **1989**, *61*, 708.
(21) Masel, R. I. *Principles of Adsorption and Reaction on Solid Surfaces;* Wiley and Sons: New York, 1996, and references therein.
(22) Ammann, M.; Baltensperger, U.; Bochert, U. K.; Eichler, B.; Gäggeler, H. W.; Jost, D. T.; Türler, A.; Weber, A. P. *J. Aerosol Sci.* **1995**, *26*, 61.
(23) Weingartner, E.; Baltensperger, U.; Burtscher, H. *Environ. Sci. Technol.* **1995**, *29* 2982.